Proceedings of the 2013 International Symposium on Liquid Metal Processing & Casting
Edited by: Matthew J. M. Krane, Alain Jardy, Rodney L. Williamson, and Joseph J. Beaman
TMS (The Minerals, Metals & Materials Society), 2013

USING A THREE-PHASE MIXED COLUMNAR-EQUIAXED SOLIDIFICATION MODEL TO STUDY MACROSEGREGATION IN INGOT CASTINGS: PERSPECTIVES AND LIMITATIONS

M. Wu[1,2], J. Li[1,2], A. Kharicha[1,2], A. Ludwig[2]
[1] Christian Doppler Laboratory for Advanced Process Simulation of Solidification and Melting, Univ. of Leoben, Austria
[2] Chair of Simulation and Modelling of Metallurgical Processes, Univ. of Leoben, Austria

Keywords: Steel, Ingot Casting, Macrosegregation, Multiphase Simulation

Abstract

A three-phase model for mixed columnar-equiaxed solidification was recently developed. The most critical features, necessary for modelling the macrosegregation, were considered: the progressive growth of the columnar dendrite trunks from the ingot surface, the nucleation and growth of the equiaxed crystals including the motion of the equiaxed crystals, the thermal and solutal buoyancy flow and its interactions with the growing crystals (equiaxed and columnar), the transport of solute due to melt convection and equiaxed sedimentation, and the columnar-to-equiaxed transition (CET). Application of the aforementioned model is mainly limited by two factors: one is the extreme computational expense; one is the lack of reliable parameters required by the model. In order to perform a calculation of industry ingot (up to hundreds of tons) on the basis of the current computer resources, a compromise is often made between the model capability and the computational feasibility, i.e. some necessary model simplifications have to be made. In this article the ongoing efforts to scale-up the current model for industry applications are reported on.

Introduction

Most valuable experimental research on the macrosegregation in large steel ingots was performed approximately one century ago [1-2]. A series of steel ingots, scaled from a few hundred kilograms up to 172 tons, were poured and cut for segregation analysis. Primary knowledge was obtained, and a typical segregation map of the large steel ingots was drawn [3-5], as shown in Figure 1. By now, most segregation phenomena can be physically explained. Multiphase flow such as thermo-solutal convection, happening in the interdendritic and bulk regions, and crystal sedimentation during solidification are the key mechanism for the formation of segregation. The thermodynamics, solidification kinetics and thermal mechanics are also coupled with the flow phenomena, and contribute to the final segregation results.

Today due to extremely high costs these kinds of experimental trials are only carried out occasionally and with caution [6-9]. Instead, the mathematical (both analytical and numerical) modelling approach becomes a most efficient tool for this purpose. Some progress has been reviewed by other authors [9-12]. Understanding of the segregation mechanism was significantly improved by the mathematical models. Unfortunately, the patterns schematically shown in Figure 1 are still not quantitatively reproducible with sufficient details by current numerical models. The great challenge arises from the multiphase nature of the solidification phenomenon. The solution of the segregation problem demands a precise description of the multiphase flow, which occurs and interacts with the solidifying microstructure (dendritic morphology) at different length scales. From the flow dynamic point of view, at least three (hydrodynamic) phases are involved in a typical ingot casting during solidification: two moving phases (liquid and equiaxed crystals) and one stationary phase (columnar dendrite trunks). In other words, a model able to reproduce the patterns of Figure 1 needs at least to consider these three phases. However, the limitation of early computational hardware resources has prevented people from considering so many phases. A compromise has to be made between the model capability and the computational feasibility. For example, Gu and Beckermann used a mixture liquid-columnar solidification model [13] and Combeau and co-workers used a two-phase equiaxed solidification model [8] to simulate the segregation in steel ingots, and some successes were achieved.

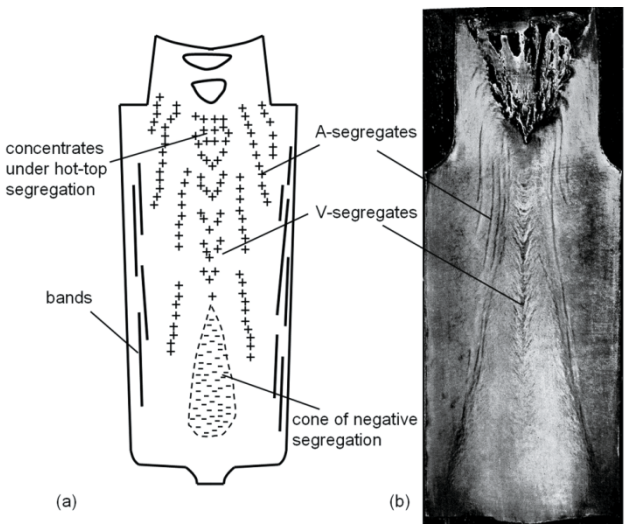

Figure 1: Typical segregation map in steel ingots (the figure is reproduced from literature [3]). (a) schematic representation with '+' for positive and '-' for negative segregation; (b) sulphur print of a 10-ton ingot.

This article does not give a comprehensive review of the topic of macrosegregation models, but focuses on the relevant activities being performed by the current authors at the University of Leoben. On the basis of previous work by Beckermann [11, 14-17], a series of multiphase solidification and macrosegregation models were proposed. These include a two-phase globular equiaxed solidification model [18-20], a two-phase monotectic solidification model [21-22], a three-phase mixed columnar-equiaxed solidification model [23-24], an equiaxed solidification model with dendritic morphology [25-26] and a five-phase mixed columnar-equiaxed solidification model with dendritic morphology [27-28]. As the computational expense increases relative to the increasing number of phases, the modelling activities take two directions. One is to further develop comprehensive models by including as many phases and physical phenomena as necessary in order to on one hand solve as much as possible segregation fea-

tures. Application of this kind of model may still rely on future enhancement of the hardware resource. On the other hand, we can base the calculations on the available hardware resource by using as simple as possible a model to solve the principal segregation phenomena of the industry ingots. This article reports on some modelling examples by using a three-phase mixed columnar-equiaxed model [23-24]. The applicability of this model to the industry ingots is investigated, and some perspectives and limitations are discussed.

Characterisation of the Three-phase Model

To characterise the three-phase mixed columnar-equiaxed solidification model, a benchmark (ϕ 66 mm x 170 mm) of a steel ingot was simulated. Macrosegregation formation due to the combined thermosolutal convection, grain sedimentation, and sedimentation-induced convection was modelled. Details about the settings for this benchmark stem from previous publications [23, 24, 29]. Model assumptions are summarised as follows:

- Solidification starts with an initial concentration Fe-0.34 wt.%C and an initial temperature of 1785 K; mould filling is ignored;
- The three phases considered are: the melt, globular equiaxed crystals and columnar dendrite trunks;
- Morphologies are approximated by step-wise growing cylinders for columnar dendrite trunks and spheres for globular equiaxed crystals;
- Columnar trunks grow from the side and bottom walls, and the columnar tip front is explicitly tracked;
- A three-parameter heterogeneous nucleation law is implemented for the nucleation of the equiaxed crystals [30]. The 3 parameters are maximum grain number density n_{max} [m^{-3}], Gaussian distribution width of nucleation ΔT_σ [K] and undercooling at the maximum grain production rate ΔT_N [K].
- Solidification shrinkage is ignored. The buoyancy force for the thermosolutal convection and crystal sedimentation is accounted for by a Boussinesq approximation;
- The equiaxed crystals ahead of the columnar tip front can move freely, but they can be captured by the columnar trunks as the local columnar volume fraction is beyond 0.2;
- Hunt's blocking mechanism [31] is applied for predicting CET (columnar-to-equiaxed transition);
- Constant heat transfer coefficients and constant ambient temperatures are assumed [23].

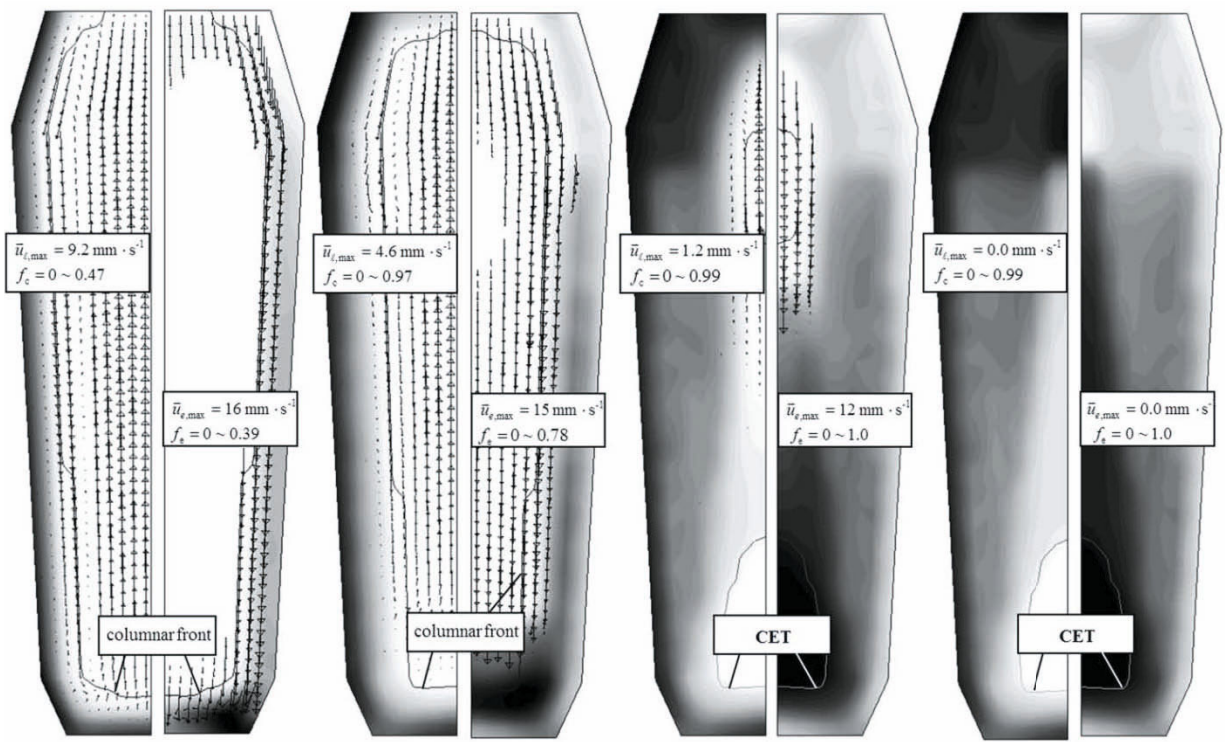

Figure 2: Simulated solidification sequence of a benchmark steel ingot. The left half of each figure shows the volume fraction of the columnar phase f_c in greyscale from minimum (bright) to maximum (black), together with the liquid velocity vectors $\bar{u}_\ell$. The right half of each figure shows the volume fraction of the equiaxed phase f_c in greyscale, together with the velocity vectors of equiaxed crystals $\bar{u}_e$. The columnar tip front and CET are indicated with a solid line. Here an arbitrary set of nucleation parameters is used to characterise the formation and sedimentation of equiaxed crystals: $n_{max} = 5\times10^9$ m^{-3}, $\Delta T_\sigma = 2$ K, $\Delta T_N = 5$ K.

The solidification sequence including sedimentation of the equiaxed crystals, the sedimentation-induced and thermosolutal buoyancy-induced melt convection are shown in Figure 2. The simulated solidification sequence agrees with the explanation of steel ingot solidification, as summarised by Campbell [32]. The columnar dendrites grow from the mould wall and the columnar tip front moves inwards. The equiaxed grains nucleate near the mould walls and in the bulk melt. The columnar dendrites are stationary, whereas the equiaxed grains sink and settle in the base region of the ingot. The accumulation of such grains at the base of the ingot

has a characteristic cone-shape. The sedimentation of grains and the melt convection influence the macroscopic solidification sequence and, thus, the final phase distribution. More equiaxed grains will be found at the bottom and in the base region, while columnar structure will be predominant in the upper part of the ingot

As the columnar tip front is explicitly tracked, the simulation shows that the columnar tip fronts from both sides tend to meet in the casting centre. However, in the lower part of the casting the accumulation of equiaxed grains stops the propagation of the columnar tip front. Its final position indicates the CET position. The CET separates the areas where only equiaxed grains appear from the areas where both columnar dendrites and equiaxed grains coexist.

The final macrosegregation pattern is predicted, as shown in Figure 3(a). From the simulation results it appears evident that the main mechanism for the cone-shaped negative segregation in the base region is the grain sedimentation. The settling grains are poor in solute elements, thus their pile-up results in negative segregation at the bottom of the ingot. A further contributing factor to the strength of negative segregation arises from the flow divergence of the residual liquid through this zone at a late solidification stage. The positive segregation at the top region of the ingot is caused by the flow of the enriched melt in the bulk region. This kind of positive segregation coincides with classical experimental results [32]. It should be noted that channel segregations, which are frequently found in large steel ingots, are not predicted in this kind of a benchmark ingot with reduced dimensions.

(a) c_{mix} (0.23 – 0.46) (b) d_c in µm (0~1000) (c) d_e in µm (394~1262)

Figure 3: Result in the finally solidified ingot. (a) Macrosegregation pattern, c_{mix} (local average concentration of columnar and equiaxed phases); (b) distribution of the columnar trunk diameter, d_c, and (c) distribution of the diameter of the equiaxed grains, d_e. The quantities are shown with grey scales from minimum (bright) to maximum (dark), together with isolines. The CET is shown by a black line.

With the given nucleation parameters n_{max} = 5. x 10^9 m^{-3}, ΔT_N = 5 K, ΔT_σ = 2 K, and a constant primary dendrite spacing of λ_1 = 1000 µm, the average equiaxed grain size d_e, and the average dendrite trunk diameter d_c, are predicted as shown in Figure 3(b)-(c). The absolute value of d_e and d_c depend on the aforementioned modelling parameters, but the predicted size distribution pattern reflects the special characteristic of the mixed columnar-equiaxed solidification. In the upper part of the ingot, the average dendrite trunk diameter has reached the maximal possible value, namely λ_1. This is due to the fact that (i) equiaxed crystals are very scarce ($f_e < 1\%$), and (ii) no interdendritic eutectic solidification was modelled in the present simulation. Contrary to the upper region, a totally equiaxed zone without any columnar dendrites exists in the area enclosed by the CET line. The cone shape distribution pattern for both d_e and d_c is similar to the pattern of the phase volume fractions f_c and f_e, as shown in Figure 2(d).

2.34-ton Ingot

The experimentally measured macrosegregation of a 2.45 ton big-end-up ingot (Fe-0.45 wt.%C) was reported [1]. The ingot had a section of square and was cast in a chilled mould. As a reference, the segregation pattern in this ingot is numerically simulated and compared with the experiment, as shown in Figure 4. Due to the lack of a precise process description, some process parameters and boundary conditions have to be derived on the basis of assumptions. The sulphur print of this ingot is shown in Figure 4(a). The measured (nominal) mixture concentration ($(c_{mix}-c_0)/c_0$) map is

shown in Figure 4(b). Configuration of this ingot, together with necessary boundary and initial conditions used for the calculation, is described in Figure 4(c). More details about the simulation configurations are presented elsewhere [33], and the same three-phase model (Section 2.0) is used. 2D axis symmetrical simulations are performed to approximate the solidification behaviour in the square section ingot. The predicted solidification sequence is shown in Figure 5 and the segregation map is shown in Figure 4(d).

The global solidification sequence in this 2.45 ton ingot (Figure 5) is actually similar to what was characterised by the previous small benchmark ingot (Figure 2-3). The sinking of the equiaxed crystals in front of the columnar dendrite tips leads to an accumulation of equiaxed phase in the base region of the ingot. The accumulation of the equiaxed phase in the base region will block the growth of the columnar dendrite tips, i.e. CET occurs there, hence finally causing a characteristic cone-shape distribution of the equiaxed zone, being enveloped in the CET line. Relatively strong negative segregation is predicted in the low-bottom equiaxed zone. With the sedimentation of a large amount of equiaxed crystals downwards, the solute-enriched melt is pushed upwards in the casting centre, hence causing a positive segregation in the upper region. Despite the above similarity between the 2.45 ton ingot (Figure 4) and the small benchmark ingot (Figure 2), significant differences are identified, which are described below.

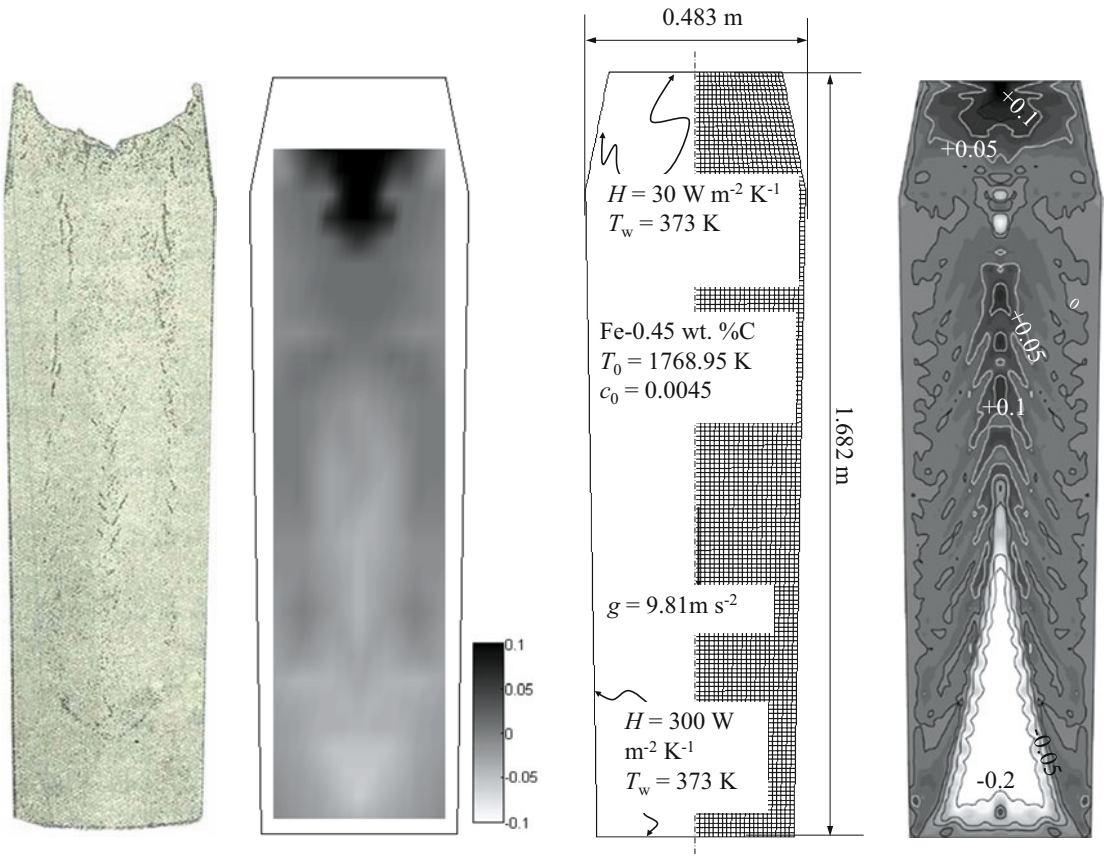

(a) sulphur print (b) measured segregation (c) B.C. and settings (d) simulated segregation

Figure 4: Configuration of a 2.45-ton industry-scale steel ingot. (a)-(b) experiment [1], (c) simulation configuration and (d) simulated macrosegregation in greyscale (black for the positive segregation and light for the negative segregation), overlapped with isolines. The macrosegregation, both experimental (b) and simulated (d), is shown for the nominal mixture concentration ((c_{mix}-c_o)/c_o). Nucleation parameters: $n_{max} = 5\times10^9$ m^{-3}, $\Delta T_\sigma = 2$ K, $\Delta T_N = 5$ K.

Firstly, the flow is much more instable (Figure 5). The melt flow in the bulk region ahead of the columnar dendrite tip front is driven by three mechanisms: the solutal buoyancy driving upwards; the thermal buoyancy driving downwards; and the equiaxed sedimentation which drags the surrounding melt downwards. Generally the two downward driving forces dominate, and the melt flows downwards along the columnar dendrite tip front. This downward flow along the columnar tips will force the melt to rise in the ingot centre. This rising melt will interact with the falling equiaxed crystals and with the downward flow near the columnar tip front, to form many local convection cells. The pattern of melt convection and crystal sedimentation becomes chaotic. These local convection cells are developed or suppressed dynamically, and the flow direction in the cells changes with time as well. The flow instability and the flow chaotic behaviour are dependent on the ingot size (ingot height). Therefore, to explain the influence of the ingot size on the macrosegregation, knowledge about the influence of the ingot size on the flow pattern is required.

Secondly, a streak-like segregation pattern (Figure 4(d)) in the mixed columnar-equiaxed region is predicted, which does not occur in the small ingot (Figure 3(5)). For a concrete explanation of this segregation pattern, a more detailed analysis of the flow and sedimentation and their interaction with the solidification is necessary; nevertheless a tentative hypothesis is proposed, as follows. As the equiaxed crystal can be captured (crystal entrap-

ment) by the growing columnar trunks, the entrapment of the equiaxed crystals will lead to a heterogeneous, i.e. streak-like, phase distribution between the columnar and equiaxed crystals immediately behind the columnar tip front, as seen in Figure 5(b)-(d). The resistance to the interdendritic flow by the columnar trunks and the entrapped equiaxed crystals is different; therefore the flow direction of the melt in this region is slightly diverted by the heterogeneous phase distribution. This diverted-flow can only be visible in the carefully zoomed view. As the macrosegregation is extremely sensitive to the interdendritic flow, it is not surprising that the induced macrosegregation (Figure 4(d)) takes the similar streak-like pattern of the phase distribution (Figure 5(d)).

One may notice that this streak-like segregation has a similar contour to the classical A-segregation, but it is still not clear if the classical A-segregation is the same as streak-like segregation or originates from this kind of streak-like segregation. According to the most widely accepted empirical explanation, A-segregation belongs to a kind of channel segregation in large steel ingots, which originates and develops in the stationary dendritic mushy zone. A recent study by the authors [34-35] in a Sn-Pb laboratory casting has found that the channel segregation can originate and develop in a pure columnar solidification, where no equiaxed crystal exists. Therefore, we name the streak-like segregation here a quasi-A-segregation. To form this quasi-A-segregation, the sedimentation of equiaxed crystals and its interaction with the columnar tip front and melt flow seem to play an important role. Details about the formation mechanism for this kind of quasi-A-segregation are still to be verified.

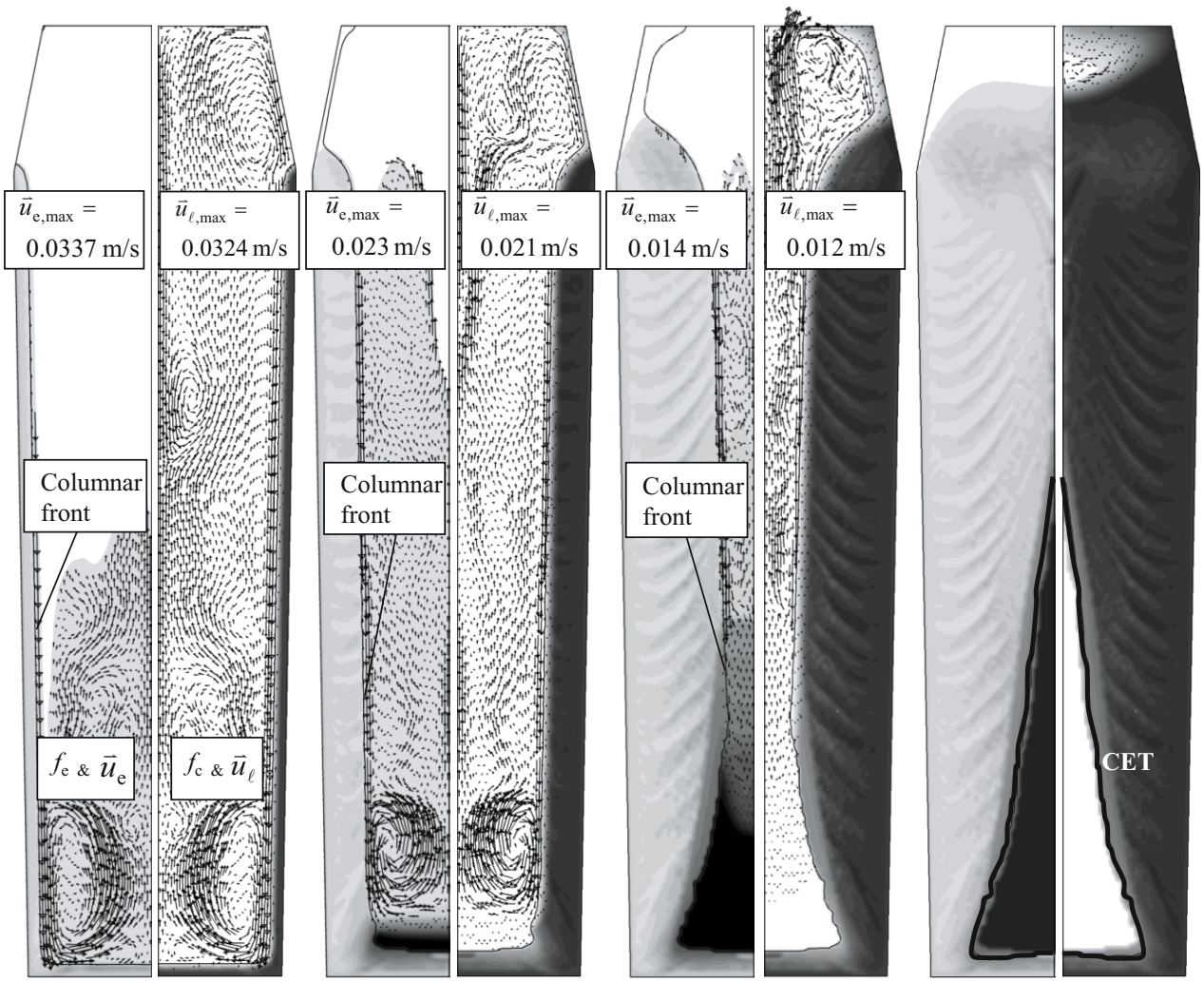

Figure 5: Solidification sequence of the 2.45-ton ingot. The volume fraction of each phase (f_e or f_c) is shown in greyscale from minimum (bright) to maximum (dark). The left half of each figure shows the evolution of the equiaxed volume fraction (f_e) together with the equiaxed sedimentation velocity ($\vec{u}_e$) in black arrows. The right half of each figure shows the evolution of the columnar volume fraction (f_c) together with the melt velocity ($\vec{u}_\ell$) in black arrows. The columnar dendrite tip position is also marked with a black solid line.

Thirdly, the simulation of the 2.45-ton ingot shows an isolated hot spot in the upper part (Figure 5(d)), which takes a long time to solidify. As the middle part of the ingot is already blocked by the columnar trunks, the solidification of the hot spot behaves like a mini-ingot. Sedimentation of the equiaxed crystals in the mini-ingot will cause a small region of negative segregation, as shown in Figure 4(d). This kind of phenomenon happens very often in long (small section) ingot casting or in the continuously-cast

round billet casting, and is called 'bridging and mini-ingotism' [36]. The experimental result of Figure 4(b) seems to show that no such 'bridging and mini-ingotism' occurs, as no such negative segregation zone is identified. It implies that the heat transfer boundary conditions applied in the current simulation might not be coincident with the reality.

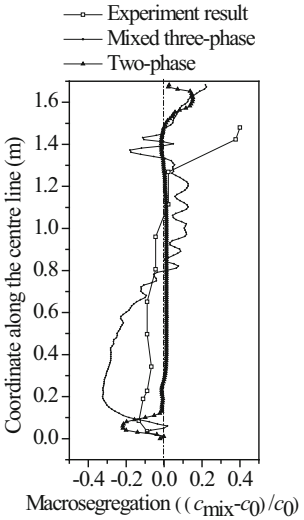

Figure 6: Comparison of the numerically predicted macrosegregation ($(c_{mix}-c_o)/c_o$) along the ingot centreline with the experiment [1]. Two simulations are performed: one is to consider the mixed columnar-equiaxed solidification ($n_{max} = 5\times10^9$ m^{-3}, $\Delta T_\sigma = 2$ K, $\Delta T_N = 5$ K); one is to ignore the occurrence of equiaxed crystal.

The segregation along the ingot centreline is analysed and compared with the experiment, as shown in Figure 6. The experiment shows the negative segregation in the lower part and positive segregation in the upper part. The model also shows the same tendency. They agree with each other qualitatively. However, the negative segregation in the lower part is predicted more severely than the experimental result. The overestimation of the negative segregation in the lower part by the model may result from two aspects. One is the assumption of globular equiaxed morphology, which can cause significant overestimation of the sedimentation-induced negative segregation. The other aspect is the error assumption of the equiaxed nucleation parameters.

In order to demonstrate the role of the equiaxed phase in the formation of segregation, an additional calculation is performed by ignoring the occurrence of the equiaxed phase. This case seems to show better agreement with the experiment, especially in the middle and lower part (Figure 6). The experimental result falls actually in a range between the two calculations. Based on the above two simulations, one may anticipate that in reality a certain amount of equiaxed crystals would appear during the solidification of this kind of a 2.45-ton ingot, but the amount of equiaxed crystals is overestimated by the current nucleation parameters.

The quantitative disagreement between the experiment and the calculations in the top part of the ingot is mainly due to the formation of the cavity, which is not considered by the current model.

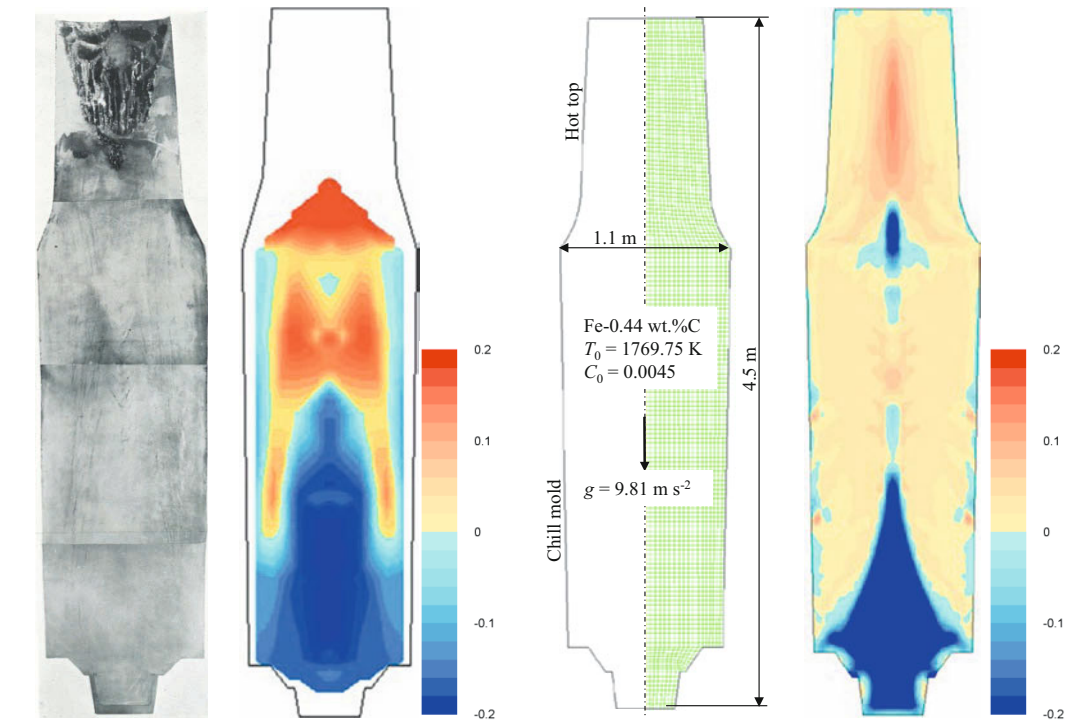

(a) etched section (b) measured segregation (c) B.C. and settings (d) simulated segregation

Figure 7: Configuration of a 25-ton industry-scale steel ingot. (a)-(b) experiment [1], (c) simulation configuration and (d) simulated macrosegregation. The macrosegregation, both experimental (b) and simulated (d), is shown for the nominal mixture concentration ($(c_{mix}-c_o)/c_o$). Nucleation parameters: $n_{max} = 5\times10^9$ m^{-3}, $\Delta T_\sigma = 2$ K, $\Delta T_N = 5$ K.

25-ton Ingot

As a further step to validate the current three-phase solidification model, a 25 ton ingot is also simulated (Figure 7). The shape of the ingot is octagonal, and the real industry alloy is multicomponent, but here only a 2D axis symmetrical calculation for a simplified binary alloy (Fe-0.44 wt.%C) is performed. Process parameters and material data have to be assumed based on the information provided by the original report [1]. Mould filling is ignored, and the nucleation parameters are assumed as: $n_{max} = 5\times10^9$ m^{-3}, $\Delta T_\sigma = 2$ K, $\Delta T_N = 5$ K. The same three-phase model as presented in Section 2 is used.

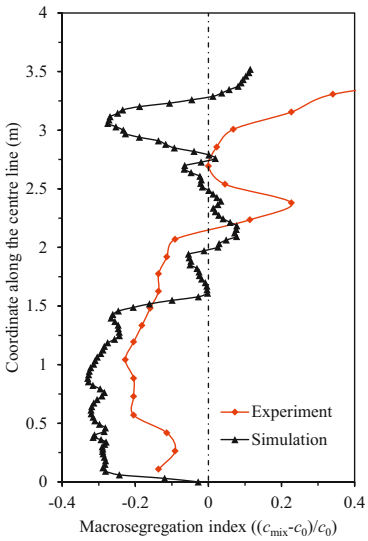

Figure 8: Comparison of the numerically predicted macrosegregation ($(c_{mix}$-$c_o)/c_o$) along the ingot centreline with the experiment [1].

The predicted macrosegregation are compared with the experimentally reported results, as shown in Figure 7 and Figure 8. Qualitatively, the predicted macrosegregation pattern follows the experimentally measured one. The bottom equiaxed zone, accompanying relatively strong negative segregation (cone shape), is predicted. This cone-shaped negative segregation is mainly due to the equiaxed crystal sedimentation. Above the tail of the cone-shaped negative segregation zone, there is a positive segregation zone. The mechanism to form such positive segregation zone is due to the transport of the solute-enriched melt in the bulk. In the upper region of the ingot, just below the hot top, when the columnar dendrite tips, growing from side walls, meet together in the casting centre, some solute-enriched melt is 'frozen' to form this positive segregation. The late solidification of the hot top behaves like a mini-ingot. Sedimentation of the equiaxed crystals continues in the mini-ingot, but the crystals can only settle in the base region of the mini-ingot, causing a secondary negative segregation zone in the mini-ingot. Finally, a large positive segregation occurs in the hot top. Segregates along the centerline (Figure 8) of both experiment and simulation show the same tendency: the negative segregation in the lower part and positive segregation in the upper part, and negative segregation region between ½ and ¾ height (just below the hot top) of the steel ingot.

Despite the above agreement, the quantitative discrepancy between numerically predicted and experimentally reported results is still significant. A cone-shaped equiaxed zone with a narrow tail extending along the centreline of the ingot is numerically predicted (Figure 7 (d)). However, the experimentally found equiaxed zone shows that the equiaxed zone is broader and it extends to a higher position, as shown in Figure 7 (a)-(b). The negative segregation in the cone-shape sedimentation zone is predicted more severely than the experimental result. The main reasons for the overestimation of the bottom negative segregation have previously been discussed: one is the deficiency of the crystal dendritic morphology, and one is the assumption of the crystal nucleation parameters. Additionally, the secondary negative segregation zone due to the mini-ingotism below the hot top is numerically predicted at a position higher than the experiment shows, and the negative segregation is predicted more intense. The reasons for this discrepancy could be the uncertainty of the thermal boundary conditions and ignorance of the formation of the shrinkage cavity in the top.

For the calculation of this 25-ton ingot, a very coarse grid (between 15 and 32 mm) was used. The number of total volume elements is 2640. The calculation time step used is between 0.01 and 0.02 s. The solidification time takes about 6.7 hours. The calculation takes about 20 days in Intel Nehalem Cluster (8 cores in parallel, 2.GHz/core). With such a coarse grid, the quasi-A-segregation cannot be calculated.

Discussions

This article related the on-going activities of the group of authors to scale-up a mixed columnar-equiaxed solidification model for industry applications. Three examples were analysed in order to evaluate the potentials and limitations of the model.

Model Potentials

Firstly, the simulated solidification sequence, the sedimentation of the equiaxed crystals, the growth of the columnar tip front and the formation of the final macroscopic phase distribution fit with the widely accepted explanations of experimental findings, as summarised by Campbell [32]: "The fragments (equiaxed grains) fall at a rate somewhere between that of a stone and snow. They are likely to grow as they fall if they travel through the undercooled liquid just ahead of the growing columnar front, possibly by rolling or tumbling down this front. The heap of such grains at the base of the ingot has a characteristic cone shape." These kinds of multiphase flow dynamics and interactions among the melt, equiaxed crystals and growing columnar trunks are the very important phenomena for modelling the segregation pattern of Figure 1. They are considered by the current model.

Secondly, it is also verified by the modelling examples above that the most typical segregates, the concentrated positive segregation under hot-top and the cone of negative segregation at the base of the ingot, can be simulated by the model. A widely accepted explanation for the formation of the cone-shaped negative segregation is verified, again in Campbell's words: "The heap of equiaxed grains at the base of the ingot has a characteristic cone shape. Because it is composed of dendritic fragments, its average composition is that of rather pure iron, having less solute than the average for the ingot." The simulated negative segregation for-

mation process by equiaxed crystal sedimentation (Figure 2 and 5) seems to have reproduced the experimental phenomenon. Mechanisms for positive segregations under the hot-top in steel ingots are diverse. It is generally agreed that they are caused by the melt convection in the bulk region or the partially solidified and/or remelted mushy zone. For example, the upper positive segregation is explained by the melt convection in the bulk region, because the light solute-rich melt rises. In actual fact, according to the recent modelling results, with the sedimentation of a large amount of equiaxed crystals downwards, the relatively positive segregated melt is pushed upwards, instead of 'rising' by itself, in the casting centre, hence causing a positive segregation zone in the upper region.

Thirdly, the possibility to calculate the distribution of the columnar and equiaxed structure has been demonstrated. The upper region of the ingot mainly consists of columnar dendrites, whereas a larger amount of equiaxed grains are predicted in the base region. Within the CET enclosed region, only the equiaxed phase exists, while outside of the CET region both columnar and equiaxed phases coexist. The macrostructure strongly depends on certain modelling and process parameters, i.e. the equiaxed nucleation parameters ΔT_N, $n_{\max}$, ΔT_σ, the primary columnar space λ_1, and boundary conditions.

Finally, the capability of the current model for the interdendritic-flow-induced channel segregation was also demonstrated [34-35], but it was not clearly shown in the above examples. The modelling result for the channel segregation is extremely sensitive to the grid resolution. Grid size less than 0.1 mm is often required, and this is unrealistic for the large industry ingots on the basis of the current computer resources. One interesting finding by the current three-phase solidification model, worth mentioning here, is the streak-like (quasi-A) segregation pattern, which occurs in such large ingots and is strengthened by the columnar-equiaxed interaction at the columnar tip front. The streak-like segregation pattern has some similarity to the classical A-segregation, but it is not clear if the classical A-segregation is the same as or whether it originates from the streak-like segregation. This is still to be verified.

Limitation of the Model

The importance of the applied process conditions, e.g. the pouring temperature, pouring method, mould materials and interfacial heat transfer between the ingot and the mould, etc., for the quantitative accuracy of the simulated solidification process and, hence, for the accuracy of the macrosegregation is evident. It is not discussed here. Following discussions focus on the aspect of numerical model.

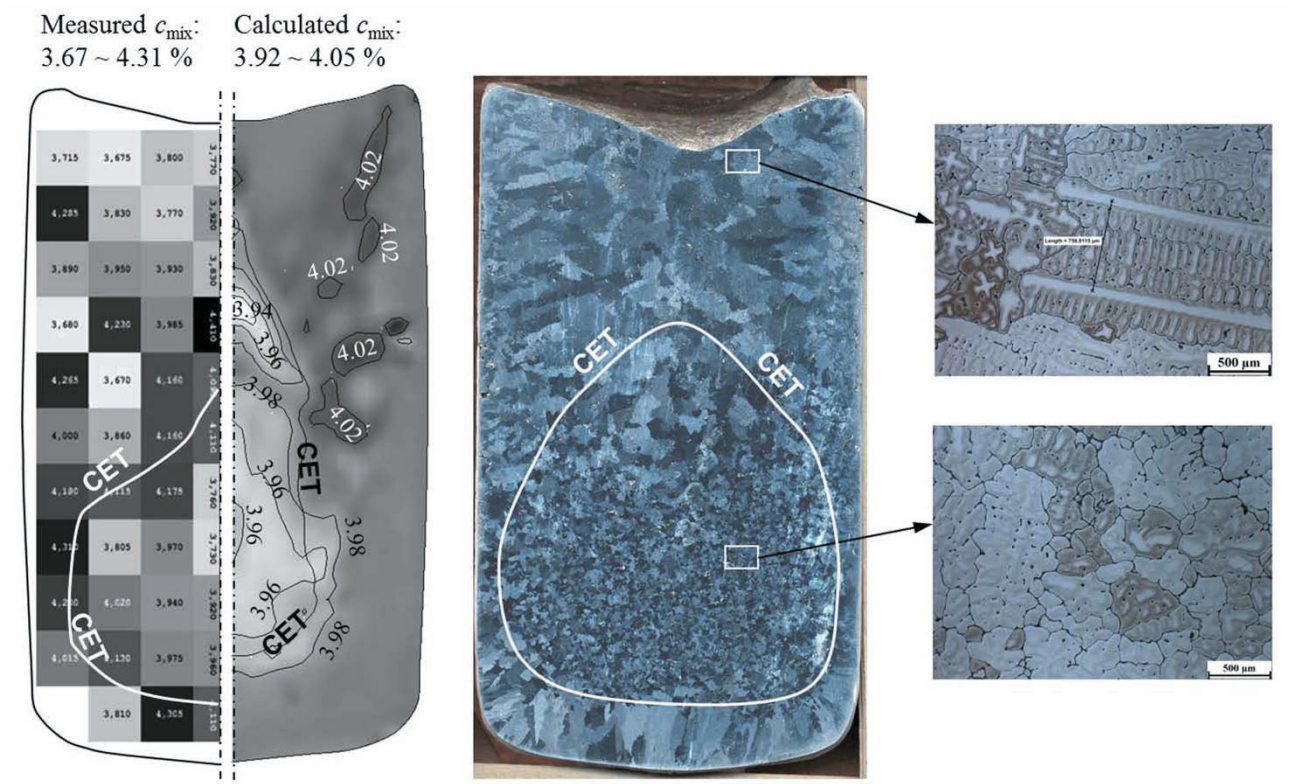

a) macrosegregation b) macrograph c) micrograph

Figure 9: An example of the modelling result of an Al-4wt.%Cu ingot with a five-phase mixed columnar-equiaxed solidification model with dendritic morphology. (a) Comparison of the measured (spark analysis) macrosegregation (left half) with the calculated one (right half). The casting is poured at 800 °C. The mixture concentration c_{mix} is shown in greyscale (dark for the highest and light for the lowest value). CET positions are plotted. This numerical simulation result shows satisfactory agreement with the as-cast macrostructure (b) macrograph, (c) micrograph.

Firstly, the influence of the nucleation event on macrosegregation was addressed in the example of the 2.45-ton ingot. The origin of the equiaxed grains may be due to different mechanisms, e.g. heterogeneous nucleation, and/or fragmentation and detachment

of dendrites by re-melting, and/or nucleation formed during pouring by contact with the initial chilling of the mould. The recent model condenses all of these phenomena into a single effective nucleation description. Here, a three-parameter heterogeneous nucleation law [30] is applied for the origin of equiaxed crystals. It is only possible to obtain the reliable nucleation parameters experimentally.

Secondly, no shrinkage cavity and porosity are considered. This deficiency will influence the accuracy of the calculation, especially in the hot-top region. As shrinkage contributes to or influences the interdendritic flow, it will also influence the final distribution of the channel segregation. However, the global segregation pattern, e.g., the concentrated positive segregation in the upper region and the cone of negative segregation at the base of the ingot, will not be significantly influenced by the shrinkage.

Thirdly, no thermal mechanics is considered. The thermal mechanical shrinkage of the solidified outer shell of the ingot will influence the internal flow, but this may not be particularly significant. What is most important is the deformation of the growing crystals due to the thermal shrinkage or the solid phase transition, which would have great impact on the flow near the end of solidification at the centreline. The 'V' segregation is very much related to this kind of deformation. This 'V' segregation is not modelled by the current model.

Finally, the current three-phase model does not include dendritic morphology. This deficiency has overestimated the cone of the negative segregation at the base, like what we see in Figure 6 and 8. In order to consider the dendritic morphology, more phases, i.e. the interdendritic melt, must be separately considered. A five-phase model was developed by the group of authors to consider the mixed columnar-equiaxed solidification with dendritic morphology [27-28]. The calculation expense is so high as to prevent application in industry ingots. The validity of this model for such a purpose has been verified, but in a laboratory Al-4.0 wt.%Cu ingot casting, as shown in Figure 9. A cylindrical casting (ϕ 75 mm x 133 mm) was poured and was analysed for both macrostructure and macrosegregation. The experimental results were used to validate the numerical simulations. Satisfactory agreement between them was obtained, as reported elsewhere [37-39].

Outlook

The future modelling activities for macrosegregation in large steel ingots will progress in two directions. One is to further enhance the model capability by including more physical phenomena such as crystal morphology, solidification shrinkage, thermal mechanics, dendrite fragmentation, etc. Another direction is to further validate and improve the existing multiphase model, and to apply it for the purposes of solving engineering problems and enhancing fundamental understanding of different segregation phenomena.

1. Thanks to the work of the Iron Steel Institute [1], many steel ingots scaled from 600 kg to 172 tons were poured and sectioned for segregation analysis. This work provides most valuable information for the validation of the numerical models. Although many process parameters for those ingots are unknown and have to be assumed, the capability to reproduce segregation patterns of all (most) those ingots numerically is an important step for the development of macrosegregation model.
2. The existing model can be applied for studying the process parameters. Despite the difficulty of quantitatively reproducing the segregation pattern of reality, the influence of the process parameters, such as casting geometry, mould materials, pouring temperature, and other engineering measures on segregation can be well described by the model. By performing this kind of a parameter study, metallurgists would acquire ideas for process optimisation.
3. Any segregation mechanism, as proposed from experimental observation, can (should) be verified quantitatively by the mathematical (numerical or analytical) model. The three-phase model can help to explain many well-known segregation phenomena in detail. It may also help to explore the new segregation phenomena, which are caused by the multiphase flow. For example, the question of streak-like segregation, here referred to as quasi-A-segregation, is raised by the authors for the first time on the basis of the current modelling result. The equiaxed-columnar interaction at the columnar dendrite tip front and its influence on the melt flow seems to induce or enhance this kind of a streak-like macrosegregation

Acknowledgements

The authors acknowledge the financial support by the Austrian Federal Ministry of Economy, Family and Youth and the National Foundation for Research, Technology and Development.

References

1. Iron Steel Institute, Report on the heterogeneity of steel ingots, *J. Iron Steel Institute*, 103 (1926), 39-151.
2. E. Marburg, "Accelerated Solidification in Ingots: Its Influence on Ingot Soundness," *J. Met*., 5 (1953), 157-172.
3. J.J. Moore and N.A. Shah, "Mechanisms of Formation of A- and V-Segregation in Cast Steel," *Int. Metals Rev*., 28 (1983), 338-356.
4. J.R. Blank and F.B. Pickering, "Effect of Solidification in Large Ingots on Segregation of Non-Metallic Inclusions, in: The Solidification of Metals," *The solidification of metals* (London: The Iron & Steel inst., 1968), 370-376.
5. H. Yamada, T. Sakurai, T. Takemonchi and K. Suzuki, "The Critical Conditions for the Formation of "A" Segregation in Forging Ingots," (Proc. Annual Meeting of AIME, Dallas, A82-39, 1982), 1-6.
6. K. Kajikawa, S. Suzuki, F. Takahashi, S. Yamamoto, T. Suzuki, S. Ueda, T. Shibata, H. Yoshida, "Development of 650-ton-class Ingot for Turbine Rotor Shaft Forging Application," (Paper presented at the 1st Int. Conf. Ingot Casting, Rolling and Forging, Session – Ingot Casting Technology, 5 June 2012, Aachen, Germany), 1-6.
7. J. Wang, P. Fu, H. Liu, D. Li, Y. Li, "Shrinkage Porosity Criteria and Optimized Design of a 100-ton $30Cr_2Ni_4MoV$ Forging Ingot," *Mater. Design*, 35 (2012), 446-456.
8. H. Combeau, M. Zaloznik, S. Hans and P.E. Richy, "Prediction of Macrosegregation in Steel Ingot: Influence of the Motion and the Morphology of Equiaxed Grains," *Metall. Mater. Trans.*, 40B (2009), 289-304.
9. G. Lesoult, "Macrosegregation in Steel Strands and Ingots: Characterization, Formation and Consequences," *Mater. Sci. Eng.* A, 413-414 (2005), 19-30.
10. M.C. Flemings, "Our Understanding of Macrosegregation: Past and Present,", *ISIJ Int*., 40 (2000), 833-841.

11. C. Beckermann, “Modelling of Macrosegregation: Applications and Future Needs,” *Int. Mater. Rev*., 47 (2002), 243-261.
12. I. Ohnaka, “Modeling of Microsegregation and Macrosegregation”, *ASM Handbook*, 15-*Casting*, ASM Int., USA, 136.
13. J. P. Gu, C. Beckermann, “Simulation of Convection and Macrosegregation in a Large Steel Ingot,” *Metall. Mater. Trans*., 30A(1999), 1357-1366.
14. J. Ni, C. Beckermann, “A Volume-Averaged Two-Phase Model for Solidification Transport Phenomena,” *Metall. Mater. Trans*., 22B (1991), 349-361.
15. C.Y. Wang, C. Beckermann, “A multiphase solute diffusion model for dendritic alloy solidification,” *Metall. Trans*., 24A (1993), 2787-2802.
16. C. Beckermann, R. Viskanta, “Mathematical Modeling of Transport Phenomena during Alloy Solidification,” *Appl. Mech. Rev*., 46 (1993), 1-27.
17. C.Y. Wang, C. Beckermann, “Equiaxed Dendritic Solidification with Convection: Part I. Multi-Scale/-Phase Modeling,” *Metall. Mater. Trans*., 27A (1996), 2754-2764.
18. M. Wu, A. Ludwig, A. Bührig-Polaczek and P. Sahm, “Influence of Convection and Grain Movement on Globular Equiaxed Solidification,” *Int. J. Heat Mass Transfer*, 46 (2003), 2819.
19. A. Ludwig, M. Wu, “Modeling of Globular Equiaxed Solidification with a Two-Phase Approach,” *Metall. Mater. Trans*., 33A (2002), 3673-3683.
20. M. Wu, A. Ludwig, J. Luo, “Numerical Study of the Thermal-Solutal Convection and Grain Sedimentation during Globular Equiaxed Solidification,” *Mater. Sci. Forum*, 475-479 (2005), 2725-2730.
21. M. Wu, A. Ludwig, L. Ratke, “Modeling of Marangoni Induced Droplet Motion and Convection during Solidification of Hypermonotectic Alloys,” *Metall. Mater. Trans.*, 34A (2003), 3009-19.
22. M. Wu, A. Ludwig, L. Ratke, “Modelling the solidification of hypermonotectic alloys,” *Modell. Simu. Mat. Sci. Eng*., 11 (2003), 755-769.
23. M. Wu, A. Ludwig, “A 3-Phase Model for Mixed Columnar-Equiaxed Solidification,” *Metall. Mater. Trans*., 37A (2006), 1613-1631.
24. M. Wu, A. Ludwig, “Using a Three-Phase Deterministic Model for the Columnar-to-Equiaxed Transition (CET),” *Metall. Mater. Trans*., 38A (2007), 1465-1475.
25. M. Wu, A. Ludwig, “Modeling Equiaxed Dendritic Solidification with Melt Convection and Grain Sedimentation, Part I: The Model,” *Acta Mater*., 57 (2009), 5621-5631.
26. M. Wu, A. Ludwig, “Modeling Equiaxed Dendritic Solidification with Melt Convection and Grain Sedimentation, Part II: The Results and Verifications,” *Acta Mater*., 57 (2009), 5632-5644.
27. M. Wu, A. Fjeld, A. Ludwig, “Modeling Mixed Columnar-Equiaxed Solidification with Melt Convection and Grain Sedimentation-Part I: Model Description,” *Comp. Mater. Sci*., 50 (2010), 32-42.
28. M. Wu, A. Fjeld, A. Ludwig, “Modeling Mixed Columnar-Equiaxed Solidification with Melt Convection and Grain Sedimentation-Part II: Illustrative Modeling Results and Parameter Studies,” *Comp. Mater. Sci*., 50 (2010), 43-58.
29. M. Wu, L. Könözsy, A. Ludwig, W. Schützenhöfer, R. Tanzer, “On the Formation of Macrosegregations in Steel Ingot Castings,” *Steel Res. Int*., 79 (2008), 637-644.
30. M. Rappaz, “Modeling of Microsegregation Formation in Solidification Processes,” *Int. Mater. Rev*., 34 (1989), 93-122.
31. J.D. Hunt, “Steady State Columnar and Equiaxed Growth of Dendrites and Eutectic,” *Mater. Sci. Eng*., 65 (1984), 75-83.
32. J. Campbell, *Castings* (Butterworth Heinemann Ltd, Oxford, 1991).
33. J. Li, M. Wu, A. Ludwig, A. Kharicha, “Modelling Macrosegregation in a 2.45 Ton Steel Ingot,” *IOP Conf. Series: Mater. Sci. Eng.*, 27 (2012), doi: 10.1088/1757-899X/33/1/012091.
34. J. Li, M. Wu, J. Hao, A. Ludwig, “Simulation of Channel Segregation Using a Two-Phase Columnar Solidification Model, Part I: Model Description and Verification,” *Comp. Mater. Sci*., 55 (2012), 407-418.
35. J. Li, M. Wu, J. Hao, A. Kharicha, A. Ludwig, “Simulation of Channel Segregation Using a Two-Phase Columnar Solidification Model, Part II: Mechanism and Parameter Study,” *Comp. Mater. Sci.*, 55 (2012), 419-429.
36. J.J. Moore, “Review of Axial Segregation in Continuously Cast Steel,” *Iron and Steel Soc*., 3 (1984), 11-20.
37. M. Wu, G. Nunner, A. Ludwig, J.H. Li, P. Schumacher, “Evaluation of a Mixed Columnar-Equiaxed Solidification Model with Laboratory Castings,” *IOP Conf. Series: Mater. Sci. Eng.*, 27 (2011), doi: 1088/1757-899X/27/1/012018.
38. M. Wu, M. Ahmadein, A. Ludwig, A. Kharicha, J.H. Li, P. Schumacher, “Simulation of the As-Cast Structure of Al-4.0wt.%Cu Ingots with a 5-Phase Mixed Columnar-Equiaxed Solidification Model,” *IOP Conf. Series: Mater. Sci. Eng.*, 27 (2012), doi: 10.1088/1757-899X/33/1/012075.
39. M. Ahmadein, M. Wu, A. Ludwig, A. Kharicha, J.H. Li, P. Schumacher, “Prediction of the As-Cast Structure of Al-4.0 wt.% Cu Ingots,” *Metall. Mater. Trans*., 44 (2013), 2895-2903.